Cerebral Cortex Advance Access published August 30, 2010

Cerebral Cortex
doi:10.1093/cercor/bhq151

A Neuronal Basis for Task-Negative Responses in the Human Brain

Pan Lin[1], Uri Hasson[1,2], Jorge Jovicich[1,2] and Simon Robinson[1]

[1]Center for Mind/Brain Sciences, University of Trento, 38100 Mattarello, Italy, and [2]Department of Cognitive and Education Sciences, University of Trento, 38068 Rovereto, Italy

Jorge Jovicich and Simon Robinson contributed equally to this work.

Address correspondence to Simon Robinson, High Field Magnetic Resonance Centre of Excellence, University of Vienna, Lazarettgasse 14, A-1090 Wien, Austria. Email: simon.robinson@meduniwien.ac.at.

Neuroimaging studies have revealed a number of brain regions that show a reduced blood oxygenation level–dependent (BOLD) signal during externally directed tasks compared with a resting baseline. These regions constitute a network whose operation has become known as the default mode. The source of functional magnetic resonance imaging (fMRI) signal reductions in the default mode during task performance has not been resolved, however. It may be attributable to neuronal effects (neuronal firing), physiological effects (e.g., task vs. rest differences in respiration rate), or even increases in neuronal activity with an atypical blood response. To establish the source of signal decreases in the default mode, we used the calibrated fMRI method to quantify changes in the cerebral metabolic rate of oxygen ($CMRO_2$) and cerebral blood flow (CBF) in those regions that typically show reductions in BOLD signal during a demanding cognitive task. CBF:$CMRO_2$ coupling during task-negative responses were linear, with a coupling constant similar to that in task-positive regions, indicating a neuronal source for signal reductions in multiple brain areas. We also identify, for the first time, two modes of neuronal activity in this network; one in which greater deactivation (characterized by metabolic rate reductions) is associated with more effort and one where it is associated with less effort.

Keywords: calibrated fMRI, default mode network, physiological artifacts, task-independent deactivation, task-negative BOLD response

Introduction

The default mode network (DMN) denotes a group of brain regions that show higher activity during rest (or nonspecific baseline conditions) than during a range of cognitive tasks (Shulman et al. 1997; Mazoyer et al. 2001; Raichle et al. 2001; McKiernan et al. 2003). Originally identified in a meta-analysis of positron emission tomography (PET) studies (Shulman et al. 1997), the network is observable both during task processing and the resting state (Beckmann et al. 2005; Damoiseaux et al. 2006; De Luca et al. 2006; Calhoun et al. 2008; Hasson et al. 2009). It is also reflected in anatomical connections (Greicius et al. 2009; van den Heuvel et al. 2009). The finding that the DMN is disrupted in Alzheimer's disease and a number of other neurological conditions (Greicius et al. 2004; Buckner et al. 2008; Broyd et al. 2009) has contributed to an explosion of interest into the function of this baseline brain activity. An enduring question underlying these investigations is whether the blood oxygenation level–dependent (BOLD) signal changes observed in the DMN during task performance are actually neuronal in origin or whether they reflect the contribution of various factors that are known to modulate the BOLD response, for example, respiration rate variations, signal related to heart rate, vascular effects, or activation with an atypical hemodynamic response.

The brain regions initially identified by Shulman et al. (1997) as showing consistent decreases in blood flow in PET during visual processing epochs relative to rest periods include an extended medial strip in frontal cortex and anterior cingulate cortex, the junction of the posterior cingulate cortex (PCC)/precuneus, and bilateral inferior parietal cortices and the amygdala-hippocampal complex (Robinson et al. 2008).

In addition to the generalized task-induced signal reductions observed in the DMN during task, several cases of negative BOLD responses have been documented for specific regions during the performance of particular tasks, including the occipital cortex for visual attention tasks (Tootell et al. 1998; Smith et al. 2000) and the ipsilateral primary sensorimotor cortex during sequential finger apposition (Allison et al. 2000). It has been postulated that the reduced activity could arise from a task-induced reduction in neuronal activation, neuronal inhibition, or redistribution of the blood supply during the visual task (Haxby et al. 1994; Shmuel et al. 2002). Using interleaved perfusion–BOLD measurements, Shmuel et al. (2002) showed that a reduction in task-specific neuronal activity is a significant contributor to the negative visual BOLD signal. Likewise, Stefanovic et al. (2004) used the calibrated functional magnetic resonance imaging (fMRI) approach to demonstrate that in motor regions, task-specific negative BOLD response is primarily attributable to neuronal deactivation. Considering baseline effects and applying calibrated fMRI, Pasley et al. (2007) showed that in the visual cortex, negative BOLD responses reflected decreases in activation rather than blood stealing or other hemodynamic artifacts.

While these studies have shown that task-dependent deactivation in visual and motor cortices is predominantly neuronal in origin and not driven by vascular steal (Shmuel et al. 2002; Hansen et al. 2004; Stefanovic et al. 2004; Pasley et al. 2007), the results cannot in principle be extrapolated as a general explanation for responses in the DMN. The reason for this is that the DMN is a network that is strongly responsive during performance of high-level cognitive tasks (as opposed to simply low-level visual and motor activity) and is a highly distributed network, the function of which has yet to be conclusively determined. In the absence of a calibrated fMRI study into deactivation of the DMN, it has been difficult to derive conclusions about the source of these task-negative responses.

There has also been a reemergence of controversy regarding deactivation in the DMN in the light of several studies showing that the distribution of DMN regions overlaps with the distribution of regions whose BOLD patterns show sensitivity to respiration- and cardiac-induced variation (Wise

et al. 2004; Birn et al. 2006; Shmuel et al. 2007; Chang et al. 2009; van Buuren et al. 2009). This poses an alternative explanation for task-negative responses in the DMN, which is grounded in changes in physiology rather than activation.

To summarize, although prior work has ruled out vascular steal as a mechanism for deactivation in sensory cortices, little is known about the cause of the task-negative response in the DMN. We therefore examined whether deactivation in this network is driven by reduction in neural/metabolic processes during task or whether it has an entirely different physiological basis.

We consider the following explanations for the observation of task-induced deactivation (TID) of the DMN and attempt to distinguish between them with the first application of quantitative fMRI to this phenomenon. First, the observed BOLD signal reductions could be related to a decrease in DMN neuronal activation that is introduced by task performance. If this were the case, these negative changes in BOLD would result from a similar coupling of changes in the cerebral metabolic rate of oxygen ($CMRO_2$), cerebral blood volume (CBV), and cerebral blood flow (CBF) as is observed in the positive BOLD response. Second, deactivations could arise from a reallocation of blood flow to neighboring activated regions ("vascular steal"). Third, deactivations could reflect neuronal activation patterns that are associated with an increase in $CMRO_2$ without the usual overcompensatory increase in CBF. Finally, task-negative BOLD changes could be related to physiological processes. Recent studies have shown that variation in respiration rate leads (because of changes in the arterial level of the vasodilator CO_2) to BOLD signal changes in regions that overlap substantially with the DMN (Birn et al. 2006). Respiratory differences between task and rest states could lead to a negative BOLD signal, manifesting as TID, if breathing was correlated with the task, as is often the case (Farthing et al. 2007; Birn et al. 2009). Fortunately, the various explanations presented above are associated with different metabolic processes. This makes it possible to resolve the underlying cause of TID in the DMN by analyzing the coupling of CBF and $CMRO_2$ using the calibrated BOLD approach, as we explain below.

A positive linear relation between CBF and $CMRO_2$ has been demonstrated in the visual (Hoge et al. 1999a), sensorimotor (Kastrup et al. 2002), and primary sensory cortices (Fox and Raichle 1986). Linearity in $CMRO_2$/CBF is therefore considered a general feature of the vascular response to neural activation. In contrast, the relationship between $CMRO_2$ and CBF during BOLD changes caused by non-neuronal factors is quite different. Hypercapnia, for instance, is generally considered to engender large changes in CBF, with $CMRO_2$ remaining mostly constant (Kety and Schmidt 1948; Horvath et al. 1994; Yang and Krasney 1995), depending on the hypercapnia level (Zappe et al. 2008). Similarly, when BOLD variations are driven by the vasodilatory influence of CO_2, as occurs during spontaneous respiration rate BOLD changes (Wise et al. 2004), no change in $CMRO_2$ is expected. For these reasons, the use of $CMRO_2$/CBF coupling to discriminate between neuronal and non-neural sources of BOLD signal changes has been successfully applied to both task-dependent activation (Hoge et al. 1999a; Chiarelli et al. 2007) and task-dependent deactivation (Shmuel et al. 2002; Stefanovic et al. 2004).

We hypothesized that the coupling ratio between $CMRO_2$ and CBF during deactivation of the DMN would be similar to that found during activation, indicating a dominantly neuronal origin for task-negative responses in the DMN. A substantially different but non-zero $CMRO_2$/CBF ratio would point to significant vascular steal or modified hemodynamic response. A $CMRO_2$/CBF ratio close to zero would indicate that BOLD signal reduction in the DMN arises primarily from physiological effects such as respiration rate variation.

Materials and Methods

Participants and Task

Twelve right-handed subjects (mean age 26.1 years, 3 female) with no history of psychiatric illness or neurological disease gave written informed consent to participate in this study, which was approved by the ethics committee of the University of Trento. An arithmetic task was presented in a self-paced block design to ensure constant engagement during blocks (Greicius and Menon 2004). A maximum of 10 s was allowed for each trial, after which the next trial or rest condition (a fixation cross) was presented. Each run consisted of 3 task blocks, which were 60–70 s long, depending on when the response to the last trial was given, and 4 rest blocks of 60 s. The average run duration was 7 min 32 s. Each subject completed 3 runs.

The arithmetic task was presented as 2 rows of numbers. The top row showed 3 numbers n_1, n_2, and n_3 belonging to a numerical series with $n_{i+1} = n_i + i \times X$, where X is the unknown non-zero integer between −100 and 100 that the subject was asked to calculate to solve the task. Subjects were asked to select which of the 2 numbers on the second row continued the series by corresponding button press. Both of the answers offered were plausible and both were either odd or even, to avoid subjects using an odd/even strategy. For example, the top row might be [41 49 65] and the bottom row [87 89], for which problem the correct answer would be 89, corresponding to $X = 8$.

Image Acquisition and Preprocessing

Images were acquired with a 4 T Bruker Medspec MRI scanner using a birdcage transmit, 8-channel receive head radiofrequency coil. Structural images were acquired using a 3D magnetization prepared rapid gradient echo optimized for gray–white matter contrast, with echo time (TE)/repetition time (TR) = 4.18/2700 ms, flip angle = 7°, isotropic 1 mm resolution, parallel imaging acceleration factor 2 (Papinutto and Jovicich 2008). Functional images were acquired using a Q2TIPS pulse arterial spin labeling sequence (Luh et al. 1999) with the following parameters: field of view = 192 mm × 192 mm, matrix size = 64 × 64, TR = 2 s, TE = 17 ms, TI1 = 700 ms, TI2 = 1400 ms, T1s = 1050 ms, flip angle = 72°, slice thickness = 7 mm, slice gap = 3 mm. Nine oblique axial slices were acquired in the AC-PC plane to cover most of the regions involved in the DMN.

Both labeled and control images are subject to BOLD weighting. In periods of stable baseline or activation, BOLD weighting of the perfusion time series is removed by subtraction of labeled images from control images. Perfusion images are contaminated by BOLD during the transition between baseline and activation states, however, as label and control are acquired with a temporal separation of TR. We minimized this BOLD contamination first by using the shortest TE possible for the Q2TIPS PICORE sequence on our magnetic resonance hardware without using parallel imaging which minimized the BOLD weighting of both labeled and control images. This echo time is both short compared with the $T2^*$ of gray matter at 4 T (~40 ms for these voxel sizes; Robinson et al. 2009) and comparable with the values used in similar studies deploying ASL sequences with EPI readouts (e.g., at 3 T of 22 ms, Stefanovic et al. 2004; 23 ms, Chiarelli et al. 2007; 25 ms, Chen and Pike 2009; and 27 ms, Luh et al. 1999; at 4 T of 26 ms, Uludag et al. 2004). Additionally, we selected a design with long task blocks so that few data points were sampled during transition phases. Finally, we used sinc subtraction of images, in which estimates are generated of the labeled signal that would have been obtained if the labeled images were acquired at the same time as the control images. This is an

effective means of reducing BOLD contamination (Aguirre et al. 2002).

Data analysis was performed using AFNI (Cox 1996) and MATLAB software written in house. The first 4 volumes of each functional run were excluded from analysis to allow for quasi-equilibrium in longitudinal magnetization to be achieved. Motion correction was performed using 3D rigid-body registration to the first retained image in each run. Images were spatially smoothed with a Gaussian kernel of 6 mm full-width at half-maximum (FWHM).

The perfusion image series was generated by sinc subtraction of the label and control images, followed by conversion to absolute CBF image series based on the kinetic model (Buxton et al. 1998). The BOLD signal was calculated by averaging adjacent tag and control images.

fMRI Data Analysis of BOLD and CBF Data

Single-subject functional activation and deactivation maps from BOLD and CBF time series were estimated using the General Linear Model. For the second-level (group) analysis, single-subject contrast maps were normalized to the Talairach coordinate reference system (Talairach and Tournoux 1988) using AFNI. Activated areas were identified using Talairach coordinates and human brain atlases (Talairach and Tournoux 1988). Multisession activation contrast maps were computed with 2-sided *t*-tests across subjects (a random effects analysis with participants as a random factor). Family-wise error (FWE) control for multiple comparisons was set at $P < 0.05$ and established using cluster-level thresholding. The single voxel level was set at $P < 0.001$ and simulations (following Forman et al. 1995 as implemented in AFNI's AlphaSim) indicated that a reliable cluster would need to exceed 5 connected voxels to be considered reliable at this FWE level.

Subject-specific regions of interest (ROIs) were defined to allow characterization of deactivations in the DMN as well as task-induced activation. ROIs defined on the basis of anatomy or BOLD activation results are liable to include draining veins that may affect the accuracy of coupling ratios, whereas CBF activation results are better localized in the parenchyma (Leontiev et al. 2007). To avoid contamination by draining veins, ROIs were defined via the overlap between suprathreshold BOLD and CBF voxels in statistical T-maps (thresholded at an uncorrected significance level of $P < 0.001$) in the PCC, left/right angular gyrus (LANG/RANG), left medial prefrontal cortex (LMPFC), left/right middle occipital gyrus (LMOG/RMOG), and left frontal inferior gyrus (LIFG). Due to higher noise in the CBF signal, CBF time courses were temporally smoothed using a Hanning filter (FWHM = 6 s) prior to calculation of percent signal changes relative to baseline.

Estimation of Functional Changes in $CMRO_2$

Relative task-induced changes in $CMRO_2$ can be calculated from relative changes in BOLD and CBF using the following relation (see Davis et al. 1998 and Hoge et al. 1999b for a derivation):

$$\frac{\mathrm{CMRO_2}}{\mathrm{CMRO_{2,0}}} = \left(1 - \frac{(\Delta \mathrm{BOLD}/\mathrm{BOLD_0})}{M}\right)^{\frac{1}{\beta}} \left(\frac{\mathrm{CBF}}{\mathrm{CBF_0}}\right)^{1-\frac{\alpha}{\beta}} \quad (1)$$

where the subscripts "0" refer to the baseline values. The parameter α describes the relationship between CBV and CBF changes, and was taken to be 0.38 (Grubb et al. 1974). The parameter β is a proportional constant related to the deoxyhemoglobin concentration in blood and was taken to be 1.3 (Buxton 2002). The parameter M is a proportional constant related to BOLD, CBF, and CBV changes and represents the maximum possible BOLD signal change that can be measured in a particular region. M has been estimated experimentally in hypercapnia studies at different field strengths (Table 1) and found to be within a range of 5.7–25 in the regions listed in the table (Uludag et al. 2004; Chiarelli et al. 2007; Leontiev and Buxton 2007; Ances et al. 2008; Restom et al. 2008). Given inherently large errors in these iso-$CMRO_2$ measurements, we follow the practice of a number of recent studies in assessing $CMRO_2$–CBF coupling over a range of M suggested by the literature (Shmuel et al. 2002; Uludag et al. 2004; Pasley et al. 2007; Lin et al. 2008; Qiu et al. 2008; Chen and Pike 2009; Wu et al. 2009). The $CMRO_2$–CBF ratio was calculated as the percent change in oxygen metabolism ($\Delta CMRO_2$) to the percent blood flow change (ΔCBF).

Results

Active and Deactive Brain Regions during a Mathematical Task

Participants in the fMRI study completed blocks of mathematical tasks that were separated by rest periods. As a validation check, we first examined patterns of activation and deactivation relative to rest during the mathematical task. These analyses were conducted separately using the BOLD and CBF data. Establishing the validity of both measures was a necessary step as $CMRO_2$ measures were derived via an equation that takes both BOLD and CBF as parameters.

Activation maps (Fig. 1) based on BOLD or CBF data were quite similar, showing the involvement of regions known from previous studies to be associated with mathematical processing (Kawashima et al. 2004; Fehr et al. 2008). Deactivation was also present in areas commonly referred to as the "default mode network" (Binder et al. 1999; Mazoyer et al. 2001). Thus, the basic findings indicate the validity of measurements in relation to prior work and demonstrate that both CBF and BOLD provide robust group-level results. On the basis of these findings, we established ROIs for subsequent analyses (see Table 2 for Montreal Neurological Institute coordinates and labels). For each of the active and deactive region, BOLD, CBF, and $CMRO_2$ changes were calculated relative to rest.

Scatter plots of BOLD and CBF signal changes in each of the ROIs considered are shown in Supplementary Figure 1. Every combination of BOLD and perfusion value corresponds to a specific rate of oxygen consumption, allowing the evaluation of the dynamic ranges of these values for different brain regions. The magnitude of BOLD signal changes observed here (around ±1%) was similar to that observed in previous studies with sensory stimuli at 3 and 4 T (e.g., ~2% in visual areas in Leontiev et al. 2007, ~1% in Ances et al. 2008) and slightly higher than that observed elsewhere with cognitive stimuli (e.g., ~0.5% in a memory task in Restom et al. 2008).

Neurovascular Coupling in Deactive Regions: Linear and Same as in Task-Active Regions

$CMRO_2$ was estimated using a validated neurovascular coupling model (eq. 1) (Davis et al. 1998). The parameter α was taken to be 0.38 (Grubb et al. 1974), and β was taken to be 1.3 (appropriate to the 4 T field strength of this study; Buxton 2002). The most suitable value of the model parameter M for 4 T is 25% (Uludag et al. 2004). This value was also adopted by Pasley et al. (2007) for their 4 T study. The CMRO2/CBF coupling ratio was estimated separately for each of the task-activated areas (RMOG, LMOG, LIFG) and for each of the deactivated areas (PCC, LANG, RANG, and LMPFC) (see Figure 2; activated areas are in plotted in red, deactivated areas in blue).

All regions—both task active and deactive—demonstrated a strong linear correlation between $CMRO_2$ and CBF (R^2 = 0.99). The coupling was found to be well described by a linear relationship, with similar slopes for all regions: 0.62 ± 0.02 (PCC), 0.60 ± 0.04 (RANG), 0.62 ± 0.05 (LANG), 0.59 ± 0.03 (LMPFC), 0.59 ± 0.02 (RMOG), 0.62 ± 0.01 (LMOG), and 0.62 ± 0.01 (LIFG). Taken together, these results show that

Table 1

$CMRO_2$:CBF coupling ratio and linear correlation (R^2) using different M values reported in the literature (with $\alpha = 0.38$, $\beta = 1.3$) in DMN deactivation areas (PCC, RANG, LANG, and LMPFC) and task-dependant activation areas (RMOG, LMOG, and LIFG)

	$CMRO_2$/CBF coupling ratios and linear correlation						
	DMN deactivation areas				Task-dependent activation areas		
	PCC	RANG	LANG	LMPFC	RMOG	LMOG	LIFG
$M = 5.7$[a]	0.47 ± 0.12 $R^2 = 0.93$	0.38 ± 0.17 $R^2 = 0.60$	0.43 ± 0.24 $R^2 = 0.26$	0.46 ± 0.13 $R^2 = 0.94$	0.47 ± 0.09 $R^2 = 0.66$	0.57 ± 0.06 $R^2 = 0.67$	0.58 ± 0.07 $R^2 = 0.37$
$M = 6.3$[b]	0.49 ± 0.11 $R^2 = 0.95$	0.41 ± 0.15 $R^2 = 0.75$	0.45 ± 0.22 $R^2 = 0.49$	0.47 ± 0.12 $R^2 = 0.96$	0.48 ± 0.08 $R^2 = 0.73$	0.58 ± 0.05 $R^2 = 0.74$	0.59 ± 0.06 $R^2 = 0.49$
$M = 7.5$[c]	0.52 ± 0.09 $R^2 = 0.97$	0.45 ± 0.13 $R^2 = 0.88$	0.49 ± 0.18 $R^2 = 0.74$	0.50 ± 0.10 $R^2 = 0.97$	0.50 ± 0.06 $R^2 = 0.82$	0.59 ± 0.04 $R^2 = 0.82$	0.59 ± 0.05 $R^2 = 0.65$
$M = 8.3$[d]	0.53 ± 0.08 $R^2 = 0.98$	0.47 ± 0.11 $R^2 = 0.92$	0.51 ± 0.16 $R^2 = 0.82$	0.51 ± 0.09 $R^2 = 0.98$	0.51 ± 0.06 $R^2 = 0.86$	0.59 ± 0.04 $R^2 = 0.86$	0.60 ± 0.05 $R^2 = 0.72$
$M = 9.2$[e]	0.55 ± 0.07 $R^2 = 0.98$	0.49 ± 0.10 $R^2 = 0.94$	0.52 ± 0.15 $R^2 = 0.87$	0.52 ± 0.08 $R^2 = 0.98$	0.52 ± 0.05 $R^2 = 0.89$	0.59 ± 0.03 $R^2 = 0.89$	0.60 ± 0.04 $R^2 = 0.78$
$M = 11.1$[f]	0.57 ± 0.06 $R^2 = 0.99$	0.52 ± 0.08 $R^2 = 0.97$	0.55 ± 0.12 $R^2 = 0.93$	0.54 ± 0.06 $R^2 = 0.99$	0.54 ± 0.04 $R^2 = 0.93$	0.60 ± 0.03 $R^2 = 0.93$	0.61 ± 0.03 $R^2 = 0.86$
$M = 25$[g]	0.62 ± 0.02 $R^2 = 0.99$	0.60 ± 0.04 $R^2 = 0.99$	0.62 ± 0.05 $R^2 = 0.99$	0.59 ± 0.03 $R^2 = 0.99$	0.59 ± 0.02 $R^2 = 0.99$	0.62 ± 0.01 $R^2 = 0.99$	0.62 ± 0.01 $R^2 = 0.99$

[a] M measured in visual cortex, 13 subjects, 21–56 years, 3 T (Ances et al. 2008).
[b] M measured in motor cortex, 6 subjects, 24–32 years, 3 T (Chiarelli et al. 2007).
[c] M measured in visual cortex, 6 subjects, 24–32 years, 3 T (Chiarelli et al. 2007).
[d] M measured in lentiform nuclei, 13 subjects, 21–56 years, 3 T (Ances et al. 2008).
[e] M measured in medial temporal lobe, 9 subjects, 21–29 years, 3 T (Restom et al. 2008).
[f] M measured in visual cortex, 10 subjects, 24–40 years, 3 T (Leontiev and Buxton 2007).
[g] M measured in visual cortex, 8 subjects, 4 T (Uludag et al. 2004).

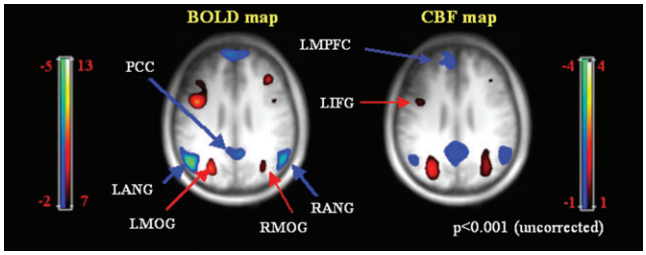

Figure 1. Functional maps of task-induced changes in BOLD (left) and CBF (right) patterns, averaged over 12 subjects. The activation (red) and deactivation (blue) maps ($P < 0.001$, t-values in color bars) are superimposed onto a T_1-weighted anatomical image in Talairach space.

Table 2

Foci of ROIs for task-activated areas (LMOG, RMOG, and LIFG) and task-deactivated areas (PCC, RANG, LANG, and LMPFC)

Region	Brodmann's area	Talairach coordinates of ROI center (BOLD)	Talairach coordinates of ROI center (CBF)
LMOG	19	−31, −70, 27	−30, −71, 27
RMOG	19	29, −63, 28	31, −67, 27
LIFG	9	−43, 4, 31	−43, 4, 31
PCC	31	−2, −56, 28	−2, −50, 28
RANG	40/39	54, −63, 28	54, −59, 28
LANG	39	−51, −66, 28	−51, −66, 28
LMPFC	9/10	−11, 56, 34	−11, 56, 34

deactivated regions in the DMN demonstrate a $CMRO_2$/CBF coupling that is identical in nature to that found in task-active regions. These results therefore provide strong support for the hypothesis that these deactivations are grounded in neural sources.

We used the most appropriate parameters in estimation of $CMRO_2$ using the neurovascular model (eq. 1) but also conducted an additional parameter sweep to determine how reliant our findings were on the values of α, β, and M, since these dictate the accuracy of $CMRO_2$ estimation (Leontiev et al. 2007). We found that the linear relationship between $CMRO_2$ and CBF and the highly similar slopes found for active and deactive areas held under a wide range of parameters values adopted for the parameters M, α, and β in the neurovascular model (ranges: $\alpha = 0.15$–0.45, $\beta = 1.0$–1.6, and $M = 5.7$–25%) (see Supplementary Figure 2 and Table 1). The value of the coupling ratio seen for deactivation was not significantly different from that for activation, except for at low values of M.

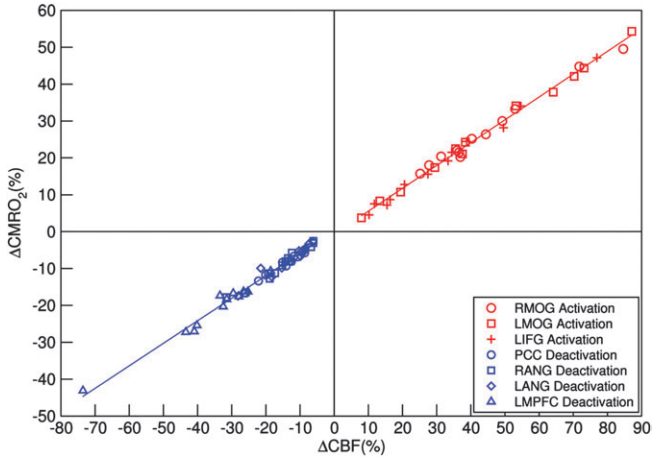

Figure 2. Neurovascular coupling between $CMRO_2$ and CBF in task-active and task-deactive regions (12 subjects). Each data point depicts $CMRO_2$ and CBF signal changes during the mathematical task relative to the resting condition for a subject in 1 ROI. Coupling ratios quoted in the main text are the results of linear fits to results for each ROI. The linear fits in this figure are over all activated regions and (separately) all deactivation regions, and are very similar to the separate ROI results.

Within-Participant Consistency of Metabolic Measures and Their Relation to Task Difficulty

Behavioral data indicated that the mathematical task required substantial effort, with relatively consistent results across the participant group: The mean accuracy in the task was 67 ± 11%

and the mean reaction time was 5290 ± 520 ms. Because $CMRO_2$ results are more directly linked to neural activity changes, we expected these to demonstrate reliable correlations between task performance parameters and the magnitude of reduced activity within the network ("deactivation" in prior literature). Activity reduction in the network typically indexes "more effortful" processing; for example, it is correlated with increased task difficulty (e.g., McKiernan et al. 2003; Pallesen et al. 2009), fewer task-unrelated thoughts (McKiernan et al. 2006), and successful subsequent memory (Otten and Rugg 2001; Anticevic et al. 2010). Thus, we expected that default mode regions would show reduced activity as a function of time on task.

In addition, we also expected to find reliable within-participant consistency in $CMRO_2$ scores across task sessions. To this end, we first tested whether participants' $CMRO_2$ results were reproducible across the 3 task sessions. Large variations across sessions would point to substantial within-participant variance and would indicate in turn that there are no strong grounds for examining the relation between $CMRO_2$ and participant behavior. Specifically, if $CMRO_2$ measures were not consistent across the 3 sessions, weak $CMRO_2$:behaviour associations would not be meaningful, and reliable effects could not be attributed to individual variance, but rather to rapidly changing transient states occurring in one run but not another. To examine this issue, we normalized participants' $CMRO_2$ scores in each ROI, for each of the 3 sessions (resulting in distributions with standard deviation [SD] approximately equal to 1, by definition, for each region and session). For each participant, we calculated the SD of the Z scores in the 3 sessions (consistency = $\sigma(Z_{1,2,3})$) and tested if this value differed from chance (i.e., consistency < 1) on the group level. In 4 of the 6 ROIs, participants demonstrated reliable consistency (LANG, LMPFC, RMOG, LMOG, $P < 0.01$). In PCC and RANG, consistency was lower than 1, though this difference was not significant at the group level ($P = 0.10$). Nonetheless, even in these regions, at least 6 participants demonstrated statistically reliable consistency across sessions ($P < 0.05$ for each of these 6 participants as determined by permutation tests), which is highly significant at the group level on a binomial test ($P < 0.00001$).

To conclude, $CMRO_2$ measures were consistent in task-active and task-deactive regions. Having established consistency, we examined whether changes in $CMRO_2$ predicted participant's behavior during task performance. To assess the relation between $CMRO_2$ and behavior, we used a regression method that is robust against univariate outliers in the data, as implemented using a robust linear model procedure (*rlm*) of the R statistical language (R Development Core Team 2009). Such robust regression methods have been proposed for analysis of both behavioral data (Wilcox 1998) and neuroimaging data (Wager et al. 2005). We correlated participants' $CMRO_2$ values obtained in the 3 sessions ($N = 36$) against their behavioral measures during those sessions. We found significant $CMRO_2$:behavior correlations in 3 areas showing deactivation (all P values <0.05 using robust regression, see Fig. 3). In the PCC and RANG, the association was negative: Metabolic activity decreases relative to rest were associated with greater task effort, as reflected by time on task and its stability. However, the LMPFC showed a positive correlation, with metabolic activity approaching that found at rest as task difficulty increased.

These results show, for the first time using metabolic measures, evidence for different functional roles being played by frontal and posterior areas. Similar analyses using the BOLD measures revealed high consistency in BOLD data across sessions, but no correlations with behavioral measures. The use of robust regression methods allows reduction of the contribution of extreme data points in a data set. For this reason, it is difficult to judge whether correlations are significantly different (i.e., construct a sampling distribution for differences between correlation values), and we can therefore not determine whether the BOLD:behavior and $CMRO_2$:behavior relations differed reliably.

Given that there was a positive correlation between $CMRO_2$ and task duration in LMPFC but this region was deactivated in all participants/sessions, we conducted a principal component analysis (PCA) to examine whether participants' $CMRO_2$ values in the LMPFC were more closely associated with activity patterns in task-active regions or task-deactive regions. To this end, we submitted all $CMRO_2$ values for each session and participant (36 sessions in all), in each of the 7 regions considered, to PCA (i.e., a 36-session × 7-region matrix). The procedure identified 2 factors with eigenvalues above 1, accounting for 66% of the variance in $CMRO_2$ values. The first factor (accounting for 40% of the variance) was positively correlated with $CMRO_2$ measures in the PCC, RANG, and LANG (0.4, 0.7, and 0.9, respectively), but negatively correlated with $CMRO_2$ measures in RMOG, LMOG, and LMPFC (–0.8, –0.6, and –0.3, respectively). Thus, this component strongly discriminated between task-active and task-deactive regions, as would be expected, but with the important exception of associating LMPFC with task-active regions in the solution (the second factor was not clearly interpretable and we do not discuss it here). The finding that activity in LMPFC is positively correlated with time on task is strongly corroborated by a recent analysis of BOLD data showing such positive correlation in a large group of subjects ($N = 252$; Yarkoni et al. 2009). Thus, even though this region is associated with reduced activity during task performance (vs. rest), its correlation pattern diverges from that found for other regions in the DMN. The PCA also implies that participants with lower $CMRO_2$ measures in "deactive" regions tended to have higher $CMRO_2$ values in active regions, with the exception of the LMPFC, which tended to cluster with active regions.

Interestingly, an identical PCA applied to the BOLD data in the 36 sessions communicated similar information, with an important caveat: This analysis (36 sessions × 7 regions) identified a first component that loaded positively and strongly on all regions. A second component loaded negatively on PCC, RANG, and LANG but positively on RMOG, LMOG, and LMPFC (jointly accounting for 60% of total variance). Thus, the second component found in the analysis of BOLD data resembles that identified in the analysis of $CMRO_2$ data. In contrast, the first highly general component identified in the BOLD data could be driven by systemic cross-subject differences in CBF, which may introduce strong correlations between BOLD data in all regions. Since CBF is partialed when deriving $CMRO_2$ values, this factor is not found in analyses of $CMRO_2$ data.

Discussion

We have investigated the sources of the common observation that large parts of the human brain appear to manifest lower

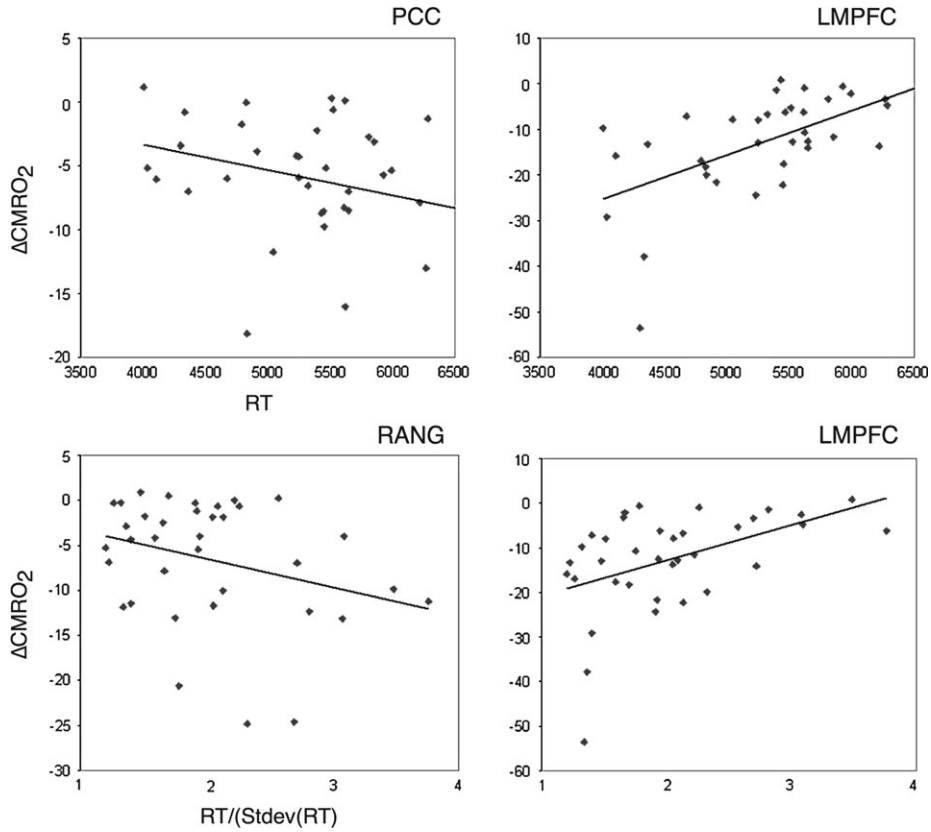

Figure 3. Correlation between metabolic activity and task performance. Three regions showing task-induced deactivation showed correlations with task performance. A correlation analysis robust against outliers demonstrated a reliable correlation (P values <0.05) between task latency and task-induced $CMRO_2$ changes in PCC and LMPFC. A reliable correlation between $CMRO_2$ changes and the coefficient of variation of task performance (RT/Stdev(RT)) was found in the RANG and LMPFC, indicating that greater consistency in response times can be manifested in either elevated or reduced $CMRO_2$ values in deactive areas.

activity during task periods than during rest when assessed using BOLD fMRI. Our results challenge recent claims that the dominant source of these deactivations may be non-neural physiological effects such as vascular steal, abnormal neurovascular coupling (Villringer and Dirnagl 1995; Shmuel et al. 2002), or task-locked fluctuations in respiratory rate (Diamond et al. 2005; Brin et al. 2006). We used calibrated fMRI in healthy subjects to determine $CMRO_2$ changes in regions showing decreased CBF during a demanding cognitive task. $CMRO_2$ is more directly correlated with neural activity than BOLD and indexes regional oxygen consumption and metabolism. Across participants, deactive regions demonstrated a linear $CMRO_2$/CBF relation, characteristic of neuronal activity. $CMRO_2$/CBF ratios were identical to those found in task-active areas. Furthermore, task-negative regions corresponded well with the task-independent deactivation areas reported in meta-analyses of deactivation effects (Shulman et al. 1997) and more recent work (Binder et al. 1999; Hutchinson et al. 1999; Mazoyer et al. 2001; McKiernan et al. 2003; Fransson 2005). Taken together, our results demonstrate a neuronal basis for the task-independent deactivation network.

To our knowledge, this is the first fMRI study to characterize sources of task-independent deactivation with perfusion MRI, and the first to use the calibrated fMRI approach to investigate the default mode. Prior work using calibrated fMRI has examined functional connectivity in resting-state networks based on $CMRO_2$ synchronization (Wu et al. 2009), or characterized $CMRO_2$/CBF neurovascular coupling in task-active regions (Hoge et al. 1999a) or in sensory regions that show deactivation under particular task contexts, but not related to the DMN (Shmuel et al. 2002; Stefanovic et al. 2004; Uludag et al. 2004; Restom et al. 2008). Our calibrated fMRI procedure was designed to compare the neurovascular coupling in task-specific activated areas with that found in DMN areas that tend to be deactive independent of particular tasks. We find that the $CMRO_2$/CBF coupling ratio in deactivated regions is essentially identical to that found in active regions, with the numeric values for the slope of the relationship (~0.6) falling within the range reported for other areas in other studies (Hoge et al. 1999a; Atkinson et al. 2000; Kastrup et al. 2002; Stefanovic et al. 2004, 2005).

The quantitative model we used to calculate $CMRO_2$ (Davis et al. 1998) incorporates parameters determined by hypercapnia studies under the assumption that carbogen breathing does not modify neuronal activity or $CMRO_2$. A recent study indicates that while neural activity is reduced during hypercapnia with 6% CO_2, it is not significantly affected by a more moderate 3% hypercapnia in the anaesthetized monkey (Zappe et al. 2008). This confirms the validity of the Davis model for the range of ΔBOLD and ΔCBF changes investigated here.

In our study, we used Grubb's equation to model the relationship between CBV and CBF (α = CBV/CBF), where α was assumed to have a constant value in space and in time. Despite the fact that we evaluated and confirmed our results

for a range of possible values of α (0.15–0.45, covering human measurements reported in the literature), in using this model there are 2 important assumptions: spatial uniformity and temporal stability. Recent human MRI (Chen and Pike 2009) and PET studies (Rostrup et al. 2005) do not reveal significant spatial variability in α, although a finer scale spatial non-uniformity might be present (as observed in animal studies; Wu et al. 2002; Jin and Kim 2008). Similarly, dynamic changes of α have recently been reported in the somatosensory cortex of anaesthetized rats studied with magnetic resonance contrast agents and single-slice fMRI during fast dynamic resolution during forepaw stimulation of different duration periods (Kida et al. 2007). These findings show that estimates of α can vary significantly between the phases of CBF rise, plateau, and decline (depending on stimulation duration). It is not yet clear whether α differs between rest, plateau, and activation (let alone during deactivation) in humans, but the study of Kida et al. shows that further work is needed to validate this aspect of the calibrated fMRI approach.

Recent studies have shown that inaccuracies can be introduced into the estimation of $CMRO_2$/CBF coupling by the parameters used to describe the neurovascular model, including the calibration constant M (Chiarelli et al. 2007). For this reason, and following the approach used in other studies, we tested the sensitivity of our results to the parameters chosen for the neurovascular model (Shmuel et al. 2002; Uludag et al. 2004; Lin et al. 2008; Schridde et al. 2008; Wu et al. 2009). We found that $CMRO_2$/CBF coupling was linear for active and deactive areas over the entire parameter space.

In considering these findings, we have used the term "deactivation" as it has been used by prior researchers who have examined task-induced signal changes in sensory (visual and motor) cortices to denote task-negative responses (Allison et al. 2000; Lustig et al. 2003; Greicius and Menon 2004; Stefanovic et al. 2004; Pasley et al. 2007). In general, the negative response we have documented may reflect decreased excitatory input or a reduction in CBF and metabolism caused by synaptic inhibition due to the interaction of γ-aminobutyric acid with its receptors (Lauritzen 2001; Gold and Lauritzen 2002). However, studies to date have used the term deactivation without implying that the processes causing task-negative responses are different from those causing task-positive responses. The DMN shows lower BOLD signal during high-demand tasks than during low-demand tasks or rest. This has, for consistency with the above convention, often been labeled TID, used as an abbreviation for both "task-induced deactivation" (McKiernan et al. 2003; Thomason et al. 2008) and "task-independent deactivation" (Shulman et al. 1997; Meyer-Lindenberg et al. 2001; Raichle et al. 2001; Laufs et al. 2003; Minzenberg et al. 2008; Yan et al. 2009). Because fMRI only offers relative measures, one cannot conclude, on the basis of fMRI information alone, whether the task state or the active state represents the "baseline" state for DMN processes. In the PET study of Raichle et al. (2001), however, absolute oxygen extraction fraction measurements indicated that localized activity decreases reflect a decrease from baseline, rather than a return to it. This would support the tendency to denote these as "task-negative" responses (i.e., deactivation). Others have chosen to see these signal changes as rest-specific activity increases (Buckner et al. 2008). In the current work, we do not make any presumptions about the nature of the underlying neuronal processes, or try to distinguish between "task-negative BOLD responses" and "rest-positive BOLD responses." Our aim was restricted to determining whether these signal changes arise due to neuronal or other causes.

Our results show that in several deactive regions, $CMRO_2$ values were associated with behavioral measures indicating more effortful task performance. In PCC and RANG, greater effort was associated with greater deactivation, supporting prior work suggesting that greater attention to task is associated with a reduced BOLD signal in these areas (McKiernan et al. 2003). Instead, the opposite pattern was observed in the medial prefrontal cortex, which was deactive for all participants but showed "reduced deactivation" (i.e., greater activation, though below baseline) for more effortful processing. In other words, as the time spent processing a task increased, $CMRO_2$ values became more similar to those at rest. This singular pattern in medial prefrontal cortex corroborates recent suggestions that it constitutes a unique node within the deactivation network. Several resting-state studies show an anterior–posterior division in the task-independent deactivation networks when the temporal characteristics of the responses are evaluated (Beckmann et al. 2005; Damoiseaux et al. 2006, 2008; Calhoun et al 2008). In addition, recent sleep studies with simultaneous electroencephalography–fMRI show that during deep sleep there is a decoupling of frontal areas from the DMN (Horovitz et al. 2009). In another work, a middle prefrontal region overlapping with the medial region identified here showed unique connectivity measures with DMN seed regions (Hasson et al. 2009): As opposed to other regions, it demonstrated stronger connectivity during task than rest, particularly for participants performing well on the task. These results suggest that medial prefrontal cortex may regulate the degree of deactivation in other regions as function of task involvement or task demands.

Finally, we note that the analyses we performed, which were based on conventional acquisitions, sensitive to the BOLD contrast, revealed similar patterns of activation and deactivation as well as strong within-participant consistency in activity across sessions. However, the BOLD data failed to reveal brain–behavior correlation patterns. Overall, our calibrated fMRI results show that deactivations patterns, when assessed via $CMRO_2$, do change as a function of interindividual differences, but the nature of these changes is nonhomogenous in the DMN, indicating functional variability among its nodes.

Taken together, our findings indicate a neuronal source for deactivation in multiple brain areas and identify for the first time two modes of neuronal activity in the DMN: one in which greater deactivation (characterized by larger metabolic rate reductions relative to rest) is associated with more effort and one where it is associated with less effort. Our results also suggest that the assessment of $CMRO_2$ or comparable indexes of neuronal activity during task and rest is important for quantifying and understanding deactivation patterns in the human brain and their implications for both healthy and clinical populations.

Funding

Government of the Provincia Autonoma di Trento, Italy, Project PAT Post-doc 2006; Fondazione Cassa di Risparmio di Trento e Rovereto; and University of Trento, Italy.

Supplementary Material

Supplementary material can be found at: http://www.cercor.oxfordjournals.org/

Notes

Conflict of Interest: None declared.

References

Aguirre GK, Detre JA, Zarahn E, Alsop DC. 2002. Experimental design and the relative sensitivity of BOLD and perfusion fMRI. Neuroimage. 15:488–500.

Allison JD, Meador KJ, Loring DW, Figueroa RE, Wright JC. 2000. Functional MRI cerebral activation and deactivation during finger movement. Neurology. 54:135–142.

Ances BM, Leontiev O, Perthen JE, Liang C, Lansing AE, Buxton RB. 2008. Regional differences in the coupling of cerebral blood flow and oxygen metabolism changes in response to activation: implications for BOLD-fMRI. Neuroimage. 39:1510–1521.

Anticevic A, Repovs G, Shulman GL, Barch DM. 2010. When less is more: TPJ and default network deactivation during encoding predicts working memory performance. Neuroimage. 49:2638–2648.

Atkinson JD, Hoge RD, Gill B, Sadikot AF, Pike GB. 2000. BOLD, CBF, and CMRO2 in the human primary motor cortex. Proceedings of the Sixth International Conference on Functional Mapping of the Human Brain, San Antonio. Neuroimage 11(5), Supplement 1. p. S803.

Beckmann CF, DeLuca M, Devlin JT, Smith SM. 2005. Investigations into resting-state connectivity using independent component analysis. Philos Trans R Soc Lond B Biol Sci. 360:1001–1013.

Binder JR, Frost JA, Hammeke TA, Bellgowan PS, Rao SM, Cox RW. 1999. Conceptual processing during the conscious resting state. A functional MRI study. J Cogn Neurosci. 11:80–95.

Birn RM, Diamond JB, Smith MA, Bandettini PA. 2006. Separating respiratory-variation-related fluctuations from neuronal-activity-related fluctuations in fMRI. Neuroimage. 31:1536–1548.

Birn RM, Murphy K, Handwerker DA, Bandettini PA. 2009. fMRI in the presence of task-correlated breathing variations. Neuroimage. 47:1092–1104.

Broyd SJ, Demanuele C, Debener S, Helps SK, James CJ, Sonuga-Barke EJ. 2009. Default-mode brain dysfunction in mental disorders: a systematic review. Neurosci Biobehav Rev. 33:279–296.

Buckner RL, Andrews-Hanna JR, Schacter DL. 2008. The brain's default network: anatomy, function, and relevance to disease. Ann N Y Acad Sci. 1124:1–38.

Buxton RB. 2002. Introduction to functional magnetic resonance imaging: principles and techniques. Cambridge (UK): Cambridge University Press.

Buxton RB, Frank LR, Wong EC, Siewert B, Warach S, Edelman RR. 1998. A general kinetic model for quantitative perfusion imaging with arterial spin labeling. Magn Reson Med. 40:383–396.

Calhoun VD, Kiehl KA, Pearlson GD. 2008. Modulation of temporally coherent brain networks estimated using ICA at rest and during cognitive tasks. Hum Brain Mapp. 29:828–838.

Chang C, Cunningham JP, Glover GH. 2009. Influence of heart rate on the BOLD signal: the cardiac response function. Neuroimage. 44:857–869.

Chen JJ, Pike GB. 2009. BOLD-specific cerebral blood volume and blood flow changes during neuronal activation in humans. NMR Biomed. 22:1054–1062.

Chiarelli PA, Bulte DP, Gallichan D, Piechnik SK, Wise R, Jezzard P. 2007. Flow-metabolism coupling in human visual, motor, and supplementary motor areas assessed by magnetic resonance imaging. Magn Reson Med. 57:538–547.

Cox RW. 1996. AFNI: software for analysis and visualization of functional magnetic resonance neuroimages. Comput Biomed Res. 29:162–173.

Damoiseaux JS, Beckmann CF, Arigita EJ, Barkhof F, Scheltens P, Stam CJ, Smith SM, Rombouts SA. 2008. Reduced resting-state brain activity in the "default network" in normal aging. Cereb Cortex. 18:1856–1864.

Damoiseaux JS, Rombouts SA, Barkhof F, Scheltens P, Stam CJ, Smith SM, Beckmann CF. 2006. Consistent resting-state networks across healthy subjects. Proc Natl Acad Sci U S A. 103:13848–13853.

Davis TL, Kwong KK, Weisskoff RM, Rosen BR. 1998. Calibrated functional MRI: mapping the dynamics of oxidative metabolism. Proc Natl Acad Sci U S A. 95:1834–1839.

De Luca M, Beckmann CF, De Stefano N, Matthews PM, Smith SM. 2006. fMRI resting state networks define distinct modes of long-distance interactions in the human brain. Neuroimage. 29:1359–1367.

Diamond J, Birn R, Bandettini P. 2005. Low frequency respiration fluctuations co-localize with 'default-mode' network. Neuroimage. 26:e549.

Farthing JP, Cummine J, Borowsky R, Chilibeck PD, Binsted G, Sarty GE. 2007. False activation in the brain ventricles related to task-correlated breathing in fMRI speech and motor paradigms. MAGMA. 20:157–168.

Fehr T, Code C, Herrmann M. 2008. Auditory task presentation reveals predominantly right hemispheric fMRI activation patterns during mental calculation. Neurosci Lett. 431:39–44.

Forman SD, Cohen JD, Fitzgerald M, Eddy WF, Mintun MA, Noll DC. 1995. Improved assessment of significant activation in functional magnetic resonance imaging (fMRI): use of a cluster-size threshold. Magn Reson Med. 33:636–647.

Fox P, Raichle M. 1986. Focal physiological uncoupling of cerebral blood flow and oxidative metabolism during somatosensory stimulation in human subjects. Proc Natl Acad Sci U S A. 83:1140–1144.

Fransson P. 2005. Spontaneous low-frequency BOLD signal fluctuations: an fMRI investigation of the resting-state default mode of brain function hypothesis. Hum Brain Mapp. 26:15–29.

Gold L, Lauritzen M. 2002. Neuronal deactivation explains decreased cerebellar blood flow in response to focal cerebral ischemia or suppressed neocortical function. Proc Natl Acad Sci U S A. 99:7699–7704.

Greicius M, Menon V. 2004. Default-mode activity during a passive sensory task: uncoupled from deactivation but impacting activation. J Cogn Neurosci. 16:1484–1492.

Greicius MD, Srivastava G, Reiss AL, Menon V. 2004. Default-mode network activity distinguishes Alzheimer's disease from healthy aging: evidence from functional MRI. Proc Natl Acad Sci U S A. 101:4637–4642.

Greicius MD, Supekar K, Menon V, Dougherty RF. 2009. Resting-state functional connectivity reflects structural connectivity in the default mode network. Cereb Cortex. 19:72–78.

Grubb RL, Jr., Raichle ME, Eichling JO, Ter-Pogossian MM. 1974. The effects of changes in PaCO2 on cerebral blood volume, blood flow, and vascular mean transit time. Stroke. 5:630–639.

Hansen KA, David SV, Gallant JL. 2004. Parametric reverse correlation reveals spatial linearity of retinotopic human V1 BOLD response. Neuroimage. 23:233–241.

Hasson U, Nusbaum HC, Small SL. 2009. Task-dependent organization of brain regions active during rest. Proc Natl Acad Sci U S A. 106:10841–10846.

Haxby J, Horwitz B, Ungerleider L, Maisog J, Pietrini P, Grady C. 1994. The functional organization of human extrastriate cortex: a PET-rCBF study of selective attention to faces and locations. J Neurosci. 14:6336–6353.

Hoge RD, Atkinson J, Gill B, Crelier GR, Marrett S, Pike GB. 1999a. Investigation of BOLD signal dependence on cerebral blood flow and oxygen consumption: the deoxyhemoglobin dilution model. Magn Reson Med. 42:849–863.

Hoge RD, Atkinson J, Gill B, Crelier GR, Marrett S, Pike GB. 1999b. Linear coupling between cerebral blood flow and oxygen consumption in activated human cortex. Proc Natl Acad Sci U S A. 96:9403–9408.

Horovitz SG, Braun AR, Carr WS, Picchioni D, Balkin TJ, Fukunaga M, Duyn JH. 2009. Decoupling of the brain's default mode network during deep sleep. Proc Natl Acad Sci U S A. 106:11376–11381.

Horvath I, Sandor NT, Ruttner Z, McLaughlin AC. 1994. Role of nitric oxide in regulating cerebrocortical oxygen consumption and

blood flow during hypercapnia. J Cereb Blood Flow Metab. 14: 503–509.
Hutchinson M, Schiffer W, Joseffer S, Liu A, Schlosser R, Dikshit S, Goldberg E, Brodie JD. 1999. Task-specific deactivation patterns in functional magnetic resonance imaging. Magn Reson Imaging. 17:1427–1436.
Jin T, Kim SG. 2008. Cortical layer-dependent dynamic blood oxygenation, cerebral blood flow and cerebral blood volume responses during visual stimulation. Neuroimage. 43:1–9.
Kastrup A, Kruger G, Neumann-Haefelin T, Glover GH, Moseley ME. 2002. Changes of cerebral blood flow, oxygenation, and oxidative metabolism during graded motor activation. Neuroimage. 15: 74–82.
Kawashima R, Taira M, Okita K, Inoue K, Tajima N, Yoshida H, Sasaki T, Sugiura M, Watanabe J, Fukuda H. 2004. A functional MRI study of simple arithmetic—a comparison between children and adults. Brain Res Cogn Brain Res. 18:227–233.
Kety SS, Schmidt CF. 1948. The effects of altered arterial tensions of carbon dioxide and oxygen on cerebral blood flow and cerebral oxygen consumption of normal young men. J Clin Invest. 27:484–492.
Kida I, Rothman DL, Hyder F. 2007. Dynamics of changes in blood flow, volume, and oxygenation: implications for dynamic functional magnetic resonance imaging calibration. J Cereb Blood Flow Metab. 27:690–696.
Laufs H, Krakow K, Sterzer P, Eger E, Beyerle A, Salek-Haddadi A, Kleinschmidt A. 2003. Electroencephalographic signatures of attentional and cognitive default modes in spontaneous brain activity fluctuations at rest. Proc Natl Acad Sci U S A. 100:11053–11058.
Lauritzen M. 2001. Relationship of spikes, synaptic activity, and local changes of cerebral blood flow. J Cereb Blood Flow Metab. 21:1367–1383.
Leontiev O, Buxton RB. 2007. Reproducibility of BOLD, perfusion, and CMRO2 measurements with calibrated-BOLD fMRI. Neuroimage. 35:175–184.
Leontiev O, Dubowitz DJ, Buxton RB. 2007. CBF/CMRO2 coupling measured with calibrated BOLD fMRI: sources of bias. Neuroimage. 36:1110–1122.
Lin AL, Fox PT, Yang Y, Lu H, Tan LH, Gao JH. 2008. Evaluation of MRI models in the measurement of CMRO2 and its relationship with CBF. Magn Reson Med. 60:380–389.
Luh WM, Wong EC, Bandettini PA, Hyde JS. 1999. QUIPSS II with thin-slice TI1 periodic saturation: a method for improving accuracy of quantitative perfusion imaging using pulsed arterial spin labeling. Magn Reson Med. 41:1246–1254.
Lustig C, Snyder AZ, Bhakta M, O'Brien KC, McAvoy M, Raichle ME, Morris JC, Buckner RL. 2003. Functional deactivations: change with age and dementia of the Alzheimer type. Proc Natl Acad Sci U S A. 100:14504–14509.
Mazoyer B, Zago L, Mellet E, Bricogne S, Etard O, Houde O, Crivello F, Joliot M, Petit L, Tzourio-Mazoyer N. 2001. Cortical networks for working memory and executive functions sustain the conscious resting state in man. Brain Res Bull. 54:287–298.
McKiernan KA, D'Angelo BR, Kaufman JN, Binder JR. 2006. Interrupting the "stream of consciousness": an fMRI investigation. Neuroimage. 29:1185–1191.
McKiernan KA, Kaufman JN, Kucera-Thompson J, Binder JR. 2003. A parametric manipulation of factors affecting task-induced deactivation in functional neuroimaging. J Cogn Neurosci. 15:394–408.
Meyer-Lindenberg A, Poline JB, Kohn PD, Holt JL, Egan MF, Weinberger DR, Berman KF. 2001. Evidence for abnormal cortical functional connectivity during working memory in schizophrenia. Am J Psychiatry. 158:1809–1817.
Minzenberg MJ, Watrous AJ, Yoon JH, Ursu S, Carter CS. 2008. Modafinil shifts human locus coeruleus to low-tonic, high-phasic activity during functional MRI. Science. 322:1700–1702.
Otten LJ, Rugg MD. 2001. When more means less: neural activity related to unsuccessful memory encoding. Curr Biol. 11:1528–1530.
Pallesen KJ, Brattico E, Bailey CJ, Korvenoja A, Gjedde A. 2009. Cognitive and emotional modulation of brain default operation. J Cogn Neurosci. 21:1065–1080.
Papinutto N, Jovicich J. 2008. Optimization of brain tissue contrast in structural images at 4T: a computer simulation and validation study. In: 25th Congress of the European Society for Magnetic Resonance in Medicine and Biology. Valencia, Spain.
Pasley BN, Inglis BA, Freeman RD. 2007. Analysis of oxygen metabolism implies a neural origin for the negative BOLD response in human visual cortex. Neuroimage. 36:269–276.
Qiu M, Ramani R, Swetye M, Rajeevan N, Constable RT. 2008. Anesthetic effects on regional CBF, BOLD, and the coupling between task-induced changes in CBF and BOLD: an fMRI study in normal human subjects. Magn Reson Med. 60:987–996.
R Development Core Team. 2009. R: a language and environment for statistical computing. In: R Foundation for Statistical Computing. Vienna, Austria.
Raichle M, MacLeod A, Snyder A, Powers W, Gusnard D, Shulman G. 2001. A default mode of brain function. Proc Natl Acad Sci U S A. 98:676–682.
Restom K, Perthen JE, Liu TT. 2008. Calibrated fMRI in the medial temporal lobe during a memory-encoding task. Neuroimage. 40: 1495–1502.
Robinson S, Barth M, Jovicich J. 2009. Fast, high resolution T2* mapping using 3D MGE and 3D EPI, with 3D correction for macroscopic dephasing effects. Proceedings of the Seventeenth Annual Meeting of the ISMRM, Toronto. Berkeley (CA): International Society for Magnetic Resonance in Medicine. p. 4525.
Robinson S, Pripfl J, Bauer H, Moser E. 2008. The impact of EPI voxel size on SNR and BOLD sensitivity in the anterior medio-temporal lobe: a comparative group study of deactivation of the Default Mode. Magn Reson Mater Phy. 21:279–290.
Rostrup E, Knudsen GM, Law I, Holm S, Larsson HB, Paulson OB. 2005. The relationship between cerebral blood flow and volume in humans. Neuroimage. 24:1–11.
Schridde U, Khubchandani M, Motelow JE, Sanganahalli BG, Hyder F, Blumenfeld H. 2008. Negative BOLD with large increases in neuronal activity. Cereb Cortex. 18:1814–1827.
Shmuel A, Yacoub E, Chaimow D, Logothetis NK, Ugurbil K. 2007. Spatio-temporal point-spread function of fMRI signal in human gray matter at 7 Tesla. Neuroimage. 35:539–552.
Shmuel A, Yacoub E, Pfeuffer J, Van de Moortele PF, Adriany G, Hu X, Ugurbil K. 2002. Sustained negative BOLD, blood flow and oxygen consumption response and its coupling to the positive response in the human brain. Neuron. 36:1195–1210.
Shulman G, Fiez J, Corbetta M, Buckner R, Miezin F, Raichle M, Petersen S. 1997. Common blood flow changes across visual tasks: II. Decreases in cerebral cortex. J Cogn Neurosci. 9: 648–663.
Smith AT, Singh KD, Greenlee MW. 2000. Attentional suppression of activity in the human visual cortex. Neuroreport. 11:271–277.
Stefanovic B, Warnking JM, Kobayashi E, Bagshaw AP, Hawco C, Dubeau F, Gotman J, Pike GB. 2005. Hemodynamic and metabolic responses to activation, deactivation and epileptic discharges. Neuroimage. 28:205–215.
Stefanovic B, Warnking J, Pike G. 2004. Hemodynamic and metabolic responses to neuronal inhibition. Neuroimage. 22:771–778.
Talairach J, Tournoux P. 2008. Co-Planar Stereotactic Atlas of the Human Brain. New York: Thieme Medical Publishers.
Thomason ME, Chang CE, Glover GH, Gabrieli JD, Greicius MD, Gotlib IH. 2008. Default-mode function and task-induced deactivation have overlapping brain substrates in children. Neuroimage. 41:1493–1503.
Tootell R, Hadjikhani N, Hall E, Marrett S, Vanduffel W, Vaughan J, Dale A. 1998. The retinotopy of visual spatial attention. Neuron. 21:1409–1422.
Uludag K, Dubowitz DJ, Yoder EJ, Restom K, Liu TT, Buxton RB. 2004. Coupling of cerebral blood flow and oxygen consumption during physiological activation and deactivation measured with fMRI. Neuroimage. 23:148–155.
van Buuren M, Gladwin TE, Zandbelt BB, van den Heuvel M, Ramsey NF, Kahn RS, Vink M. 2009. Cardiorespiratory effects on default-mode network activity as measured with fMRI. Hum Brain Mapp. 30:3031–3042.

van den Heuvel MP, Mandl RC, Kahn RS, Hulshoff Pol HE. 2009. Functionally linked resting-state networks reflect the underlying structural connectivity architecture of the human brain. Hum Brain Mapp. 30:3127–3141.
Villringer A, Dirnagl U. 1995. Coupling of brain activity and cerebral blood flow: basis of functional neuroimaging. Cerebrovasc Brain Metab Rev. 7:240–276.
Wager TD, Keller MC, Lacey SC, Jonides J. 2005. Increased sensitivity in neuroimaging analyses using robust regression. Neuroimage. 26:99–113.
Wilcox RR. 1998. How many discoveries have been lost by ignoring modern statistical methods? Am Psychol. 53:300–314.
Wise RG, Ide K, Poulin MJ, Tracey I. 2004. Resting fluctuations in arterial carbon dioxide induce significant low frequency variations in BOLD signal. Neuroimage. 21:1652–1664.
Wu CW, Gu H, Lu H, Stein EA, Chen JH, Yang Y. 2009. Mapping functional connectivity based on synchronized CMRO2 fluctuations during the resting state. Neuroimage. 45:694–701.
Wu G, Luo F, Li Z, Zhao X, Li SJ. 2002. Transient relationships among BOLD, CBV, and CBF changes in rat brain as detected by functional MRI. Magn Reson Med. 48:987–993.
Yan C, Liu D, He Y, Zou Q, Zhu C, Zuo X, Long X, Zang Y. 2009. Spontaneous brain activity in the default mode network is sensitive to different resting-state conditions with limited cognitive load. PloS One. 4:e5743.
Yang SP, Krasney JA. 1995. Cerebral blood flow and metabolic responses to sustained hypercapnia in awake sheep. J Cereb Blood Flow Metab. 15:115–123.
Yarkoni T, Barch DM, Gray JR, Conturo TE, Braver TS. 2009. BOLD correlates of trial-by-trial reaction time variability in gray and white matter: a multi-study fMRI analysis. PloS One. 4:e4257.
Zappe AC, Uludag K, Oeltermann A, Ugurbil K, Logothetis NK. 2008. The influence of moderate hypercapnia on neural activity in the anesthetized nonhuman primate. Cereb Cortex. 18: 2666–2673.